Self-Consistent Field Analysis of Grafted Star Polymers

D. J. Irvine and A. M. Mayes*

Department of Materials Science and Engineering, Massachusetts Institute of Technology, Cambridge, Massachusetts 02139

L. Griffith-Cima

Department of Chemical Engineering, Massachusetts Institute of Technology, Cambridge, Massachusetts 02139

Received December 26, 1995; Revised Manuscript Received May 11, 1996[⊗]

ABSTRACT: A self-consistent mean-field treatment of star polymers grafted to an impenetrable surface is developed and used to calculate the near-surface equilibrium segment density profiles. The effects of architecture and grafting density on molecular conformation in the absence of enthalpic interactions are explored. We find that the tethering arm of a grafted star is maximally stretched at moderate grafting density, and thus the height of a layer of stars is controlled by the distribution of chains extending from the branch node into the solvent. Evidence is presented for the existence of a "virtual surface" at the branch node of grafted stars, above which arms stretching into the solvent behave as linear brushes independently grafted to the branch node layer. Grafted layers of stars and linear chains are contrasted by comparing the total concentration profiles and end segment distributions. Results suggest that star polymers may be superior for preparing a cell adhesion substrate characterized by high surface coverage and localization of end groups near the top of the layer.

I. Introduction

Polymers tethered by one end to a surface by means of chemical grafting or end-group adsorption are of growing commercial interest for a wide range of applications such as colloidal stabilization, compatibilization at liquid−liquid and liquid−solid interfaces, "smart" gating, and biocompatible surface design.[1−5] Extensive theoretical and experimental work has shown that grafted chains are uniquely suited to prevent adsorption and particle flocculation.[1,6−12] However, realization of these properties using brushes of linear chains is impeded by the inherent difficulty in creating a dense layer of these chains. One way to circumvent this difficulty is to work with a self-assembling monolayer, but these layers lack the long-term stability of a chemically grafted layer.[13] Another option may be to change the architecture of the grafted molecule.

In this study, we have systematically explored the effects of polymer architecture on the surface concentration profile of a grafted layer of star polymers. Stars have a more compact structure and their conformations in a grafted layer are thus expected to be very different from linear polymers. Stars may thus confer advantages where a high chain segment density at the surface is needed. For example, the ability of grafted poly(ethylene oxide) (PEO) chains to resist protein adsorption has been shown to correlate with the chain segment density at the surface.[13] Grafted star PEO may enable enhanced performance of implants and tissue culture substrates by improving resistance to protein adsorption. Of further interest is the use of grafted layers, including PEO, as selectively adsorbing surfaces. A "selective" surface would resist nonspecific protein adsorption but present ligands recognized by particular cell surface receptors. Such a surface would require a high volume fraction of grafted polymer near the surface and a large density of functionalized end groups at the top of the grafted layer. The unique architecture of star polymers may be particularly suited for satisfying these criteria.

The systems investigated consist of star polymers grafted by a single tether to an impenetrable surface. The influence of molecular architecture and grafting density on the near-surface segment density profile is studied through a one-dimensional self-consistent mean-field (SCF) treatment, based on the lattice theory of Scheutjens and Fleer as extended to terminally attached chains by Cosgrove et al. and Hirz.[14−16] Results are compared with those obtained previously for linear chain brushes.

Early theoretical work on grafted linear chains by Alexander and de Gennes led to a scaling relationship for the brush height, H, based on a Flory-type free energy balance of the stretching energy in competition with a repulsive chain−chain contact energy:[9,10]

$$H \sim N\sigma^{1/3} \tag{I.1}$$

where N is the number of segments per chain and σ is the grafting density, i.e., the number of grafted chains per unit surface area. This simple model provides correct first-order predictions of H but contains no details about the distribution of chains within the brush or the concentration profile itself.[18] A more detailed analytical treatment of brushes in solvent was made independently by Milner, Witten, and Cates and by Skvortsov, Zhulina, Priamitsyn, et al.[8,17] These theories deduced the local osmotic pressure $\mu(z)$ which acts against the addition of more chain segments to the brush to be

$$\mu(z) = \text{constant} - (\pi^2/8N^2)z^2 \tag{I.2}$$

Because the energetic penalty for adding a segment is an increase in the number of chain−chain contacts, $\mu(z) \sim \phi(z)$, and a parabolic concentration profile results. Calculations were also made of the distribution of ends and the force required to compress a brush. Limited experimental studies lend support for these findings, although further refinements have been made to the brush theory as outlined in the review by Milner and more recent studies.[7,11] Further understanding of linear polymer brushes has also been aided by Monte

[⊗] Abstract published in *Advance ACS Abstracts,* August 1, 1996.

S0024-9297(95)01903-6 CCC: $12.00

Carlo, molecular dynamics, and other numerical studies.[5,12,15,16,18−23]

Carignano and Szleifer studied the layer structure of three-arm grafted chains having one arm tethered to the surface and two free arms of equal length using a single-chain mean-field theory.[22] The length N_{arm} of the grafting arm was varied along with the free arm lengths, keeping the total number of segments constant. They found that as grafting density increases, the two free arms of these polymers tend to orient antiparallel to the branch point, one arm toward the surface and one arm into the solvent. Cherepanova and Stekolnikov also examined the general structure of a layer of small star molecules ($N_{total} < 50$), using a weighted-density functional method.[23] The concentration profile in a grafted star layer was found to exhibit a plateau region of nearly constant segment density, and the tendency for the tethered arm of stars to become strongly stretched with increased grafting density was observed. In this paper, we will present results for grafted stars having much longer arms and total number of segments up to $N_{total} = 1400$, with number of arms varied between three and twelve. In addition, results for stars having both long and short arms are presented.

The values of grafting density presented, $\sigma = 0.02-0.06$, are motivated by coverages obtained with linear chains in experimental studies. Recent work by Mansfield et al.[11] and Siqueira et al.[24] showed that grafting densities $\sigma = 0.06-0.08$ chains/statistical segment area are readily achieved. Mansfield et al. adsorbed polystyrene chains of 780 repeat units to silicon oxide in a near-Θ solvent and obtained interchain distances d of 33 Å ($=0.59R_g^{ideal}$) after 2 h equilibration time. Theoretical predictions of Ligoure and Leibler[25] and Milner[26] showed that the denser equilibrium grafting density expected from considerations of chain length and adsorption energy is approached at an exponentially decaying rate beyond the point of chain overlap due to the large energy barrier presented by the chains already adsorbed at the interface. It has been recognized by several workers that moderately stretched polymer brushes can be obtained by covalently coupling chains to a substrate from a poor solvent, which strongly reduces their molecular dimensions to those of ideal chains.[1] When removed from the coupling solution and placed in a good solvent, the swollen coils overlap and are stretched perpendicular to the surface. Because star polymers swell to a greater degree in a good solvent than linear chains of equivalent ideal dimensions, one might expect a stronger degree of stretching attained in grafted layers of stars prepared in this manner.

Based on these experimental findings, we will restrict our discussion of grafting densities to $\sigma \leq 0.06$, corresponding to an interchain spacing of $d \geq 0.6R_g^{ideal}$.

The focus of this study is the effect of star architecture on layer structure. We will consider only the case of a good solvent ($\chi = 0$). Polymers in good solvents have practical application in many systems including the PEO−water system of interest to the biomaterials community. The influence of arm number, arm molecular weight, total molecular weight, grafting density, and a bimodal arm length distribution on surface concentration profiles is investigated. The concentration profiles of a grafted layer of star polymers is also contrasted with a linear polymer grafted layer, where the star and linear molecules have the same *ideal* dimensions. This comparison is relevant to the experimental situation where chains are covalently grafted in a poor solvent and subsequently swollen in a good solvent.

Section II outlines the SCF model and the calculation of the segment weighting factors for the grafted stars. Following this is a discussion of the results obtained for each of the variables in the study.

II. SCF Model

The self-consistent field lattice theory of Scheutjens and Fleer provides the criteria for determining the equilibrium volume fraction profile of a polymer system on a one-dimensional lattice.[14,27] The lattice consists of M consecutive layers with the surface adjacent to the first layer. Each layer has Z nearest neighbors; the fraction of nearest neighbors in a layer z is $\lambda_0 = 1/2$, and the fraction of neighbors in each adjacent layer $(z-1)$ and $(z+1)$ is $\lambda_1 = 1/4$. These values for λ correspond to a close-packed fcc lattice in three dimensions, which maximizes the number of arms that can be extended from the central "branch node". Interactions between segments are not treated explicitly but are accounted for by a mean-field approximation. Thus all interactions are averaged into a field which varies only in the direction perpendicular to the grafting plane. Flory−Huggins theory is used to describe the potential energy of a segment in layer z:

$$u(z)/kT = -2\chi\phi(z) - \ln(1-\phi(z)) \qquad \text{(II.1)}$$

Each star has N_{total} segments and f arms of N_{arm} segments each. The distribution of segments is found by calculating a set of Boltzmann factors for the components of the system. For single segments in a lattice, the segment weighting factor is defined by

$$G(z) = \exp(-u(z)/kT) \qquad \text{(II.2)}$$

We must, however, also account for the polymer chain connectivity, in this case, star molecules. This is done by finding the probability of a segment s on one of the star arms being located in a layer z using the definitions

$$G(z,s|\text{end}_i) = \langle G(z,s-1|\text{end}_i)\rangle G(z) \qquad \text{(II.3)}$$

$$G(z,s|\text{center}) = \langle G(z,s+1|\text{center})\rangle G(z) \qquad \text{(II.4)}$$

$$G(z,\text{end}_i|\text{end}_i) = G(z) \qquad \text{(II.5)}$$

$$G(z,\text{center}|\text{center}) = \frac{\sum_{j\neq i} G(z,\text{center}|\text{end}_j)}{(G(z))^{f-2}} \qquad \text{(II.6)}$$

The angular brackets denote a weighted average over the layer z and the two adjacent layers $(z-1)$ and $(z+1)$. The weighted average of a quantity x is defined as

$$\langle x(z)\rangle = \lambda_1 x(z-1) + \lambda_0 x(z) + \lambda_1 x(z+1) \qquad \text{(II.7)}$$

All of the quantities of interest in this system are zero at $z = 0$ and $z = M + 1$ (i.e., the lattice is bounded by hard walls). $G(z,s|\text{end}_i)$ is the statistical weight of a segment s in layer z based on the possible configurations of the chain from s to the arm end, and $G(z,s|\text{center})$ is the weight for segment s in layer z after accounting for possible configurations of the rest of the molecule from the ends of the other arms through the center node to segment s. The notations $s-1$ and $s+1$ indicate the next segment toward the arm end and the next segment toward the branch node, respectively. The multiplica-

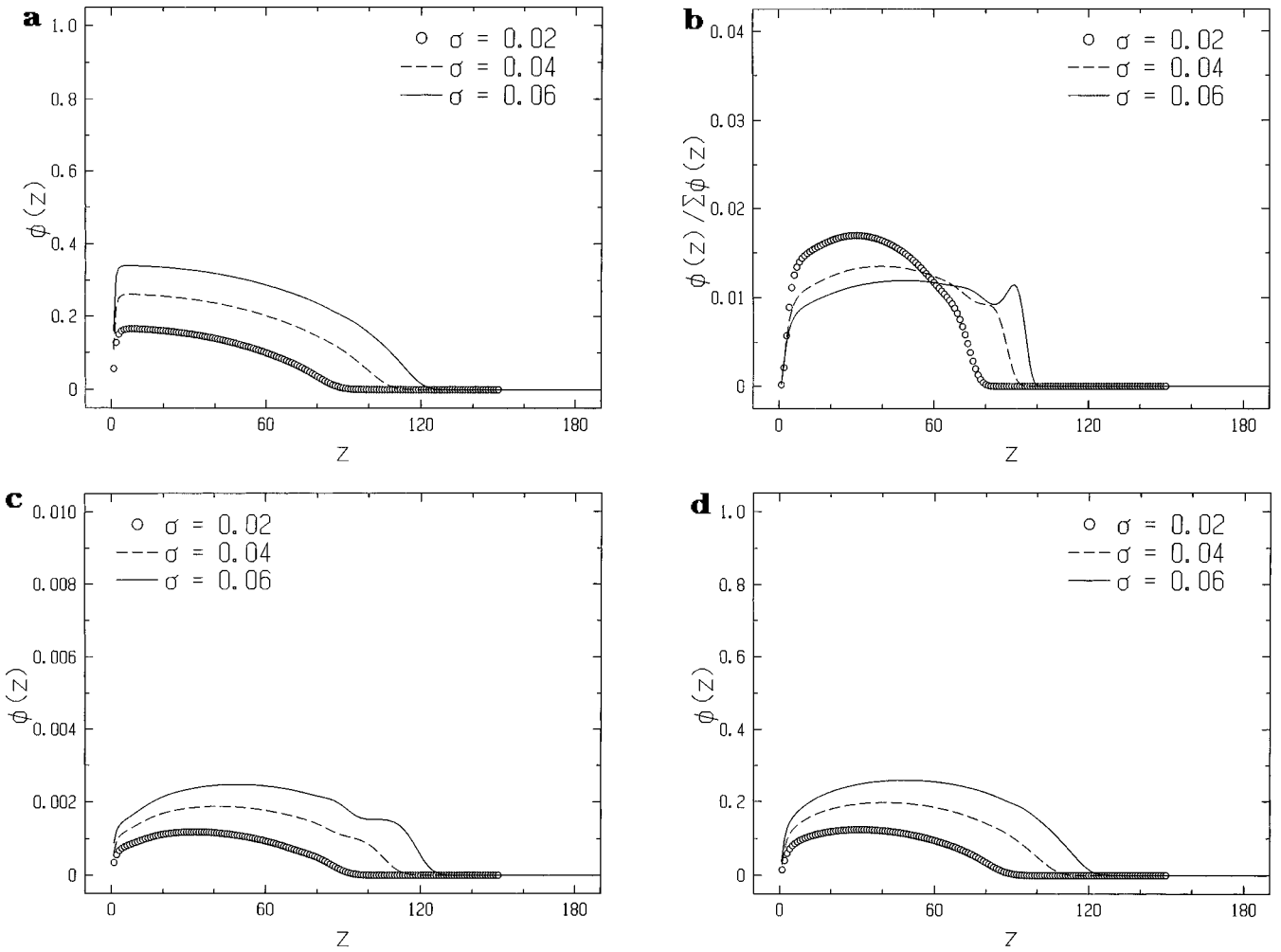

Figure 1. Volume fraction profiles for a grafted layer of five-arm star molecules tethered to the surface ($z = 0$) by a single chain. σ is the grafting density, $N_{arm} = 100$, $N_{total} = 501$. (a) Total volume fraction profiles. (b) Normalized center segment volume fraction profiles. The center segment localizes further from the surface as the tethered branch becomes stretched with increasing σ. (c) Arm end segment volume fraction profiles. (d) Arm segment volume fraction profiles.

tion in (II.6) is carried out for each of the other $f - 1$ arms; $G(z,\text{center}|\text{end}_j)$ is obtained for each arm using eqs II.3 and II.5. The division by $(G(z))^{f-2}$ is carried out to eliminate multiple counting of the center segment weight. These recursion relations can be used to build a matrix describing the segment weighting factors for the segments of each arm in all M layers.

From the Boltzmann factors, we find the volume fraction for each molecule m:

$$\phi_m(z) = C_m \sum_{s=1}^{N_{total}} \frac{G(z,s|\text{end})G(z,s|\text{center})}{G(z)} \quad \text{(II.8)}$$

where C_i is a normalization constant, obtained from the condition that each layer be filled, i.e.

$$\sum_{z=1}^{M} \sum_{m=1}^{2} \phi_m(z) = M \quad \text{(II.9)}$$

where the inner summation is over each type of molecule in the system. When the grafting density is specified, the normalization constant for the polymer becomes

$$C_{polymer} = \sigma / \sum G(z,\text{end}|\text{center}) \quad \text{(II.10)}$$

where σ is the grafting density, defined as the number of grafted molecules per unit surface area, n/A. The sum in (II.10) is over z and the factor $G(z,\text{end}|\text{center})$ is the weighting factor of a star end being located in layer z.

The volume fractions in eq II.8 must be self-consistent with the potential given by eq II.1. This gives a set of M equations and M unknowns which can be solved by standard numerical methods.[27]

III. Results and Discussion

Effect of Grafting Density. The radius of a star polymer is generally greater than the end-to-end distance of a linear chain of the same molecular weight as a star arm due to stretching of the arms that occurs near the crowded star center.[28] In addition, the density of segments near the surface for a given grafting density σ is higher for a star brush than for a linear chain brush of equivalent molecular weight due to the star's compact architecture. The combination of these two effects leads to strong stretching of the tethering arm even at low grafting densities. Volume fraction profiles are shown in Figures 1 and 2 for grafted layers of stars with five arms and ten arms, respectively, as a function of σ. For both systems $N_{arm} = 100$, with one arm tethered to the surface. The strongly stretched tethered arm is identified by the sharp peak occurring in the center segment profiles (Figure 2b) for $z = N_{arm} + 1$. This layer $z_{node} = N_{arm} + 1$ is a delimiter between the region of the arms stretching toward the surface and those stretching into

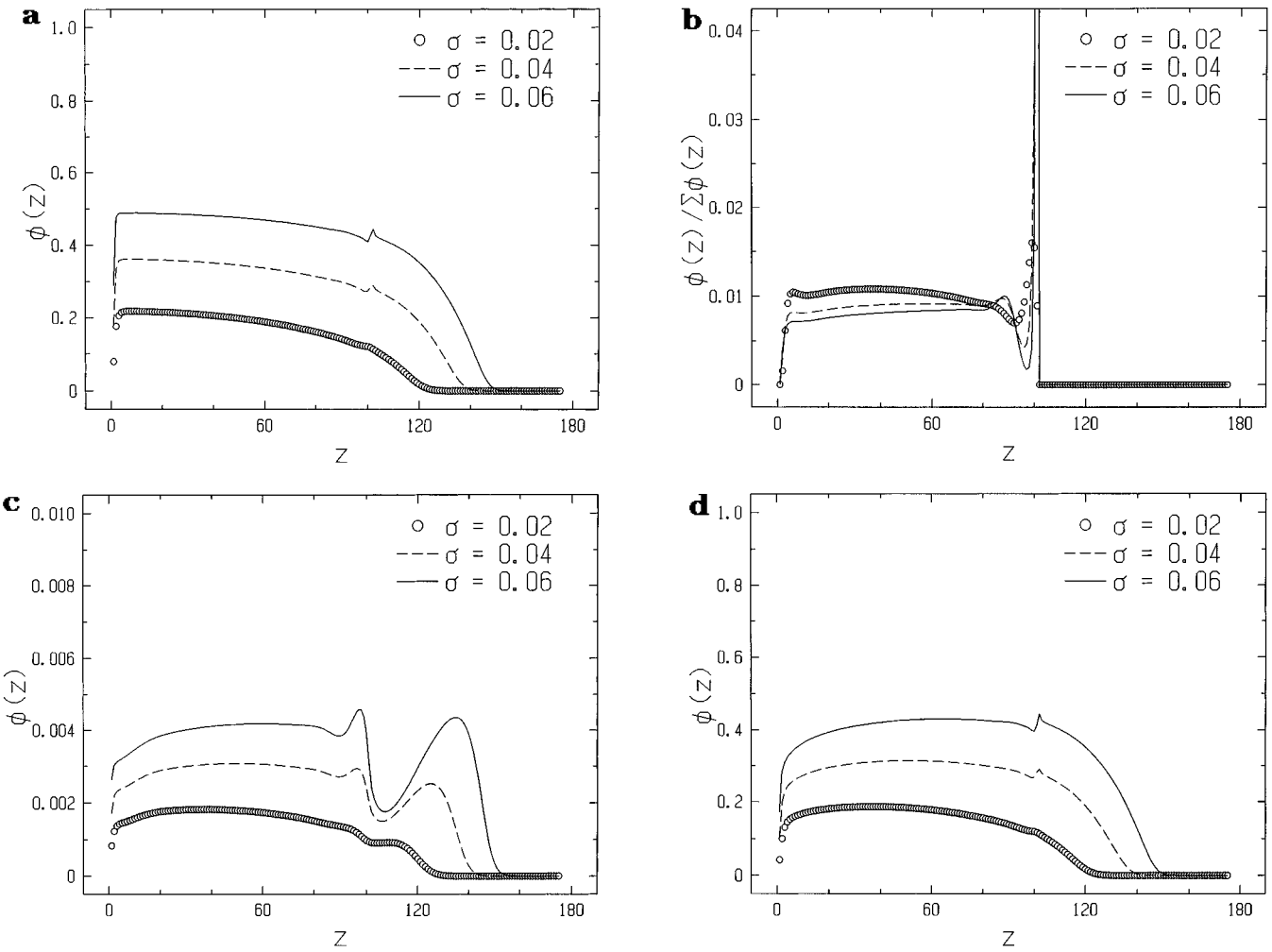

Figure 2. Volume fraction profiles for a grafted layer of ten-arm star molecules tethered to a surface ($z = 0$) by a single arm. $N_{arm} = 100$, $N_{total} = 1001$. (a) Total volume fraction profiles. (b) Normalized center segment volume fraction profiles. In this case, the tethered arm is stretched even at $\sigma = 0.02$. (c) Arm end segment volume fraction profiles. (d) Arm segment volume fraction profiles.

the solvent. As pointed out by Carignano and Szleifer[22] in their study of three-arm grafted polymers, the stretching of the tethered arm can be understood as a balance between the loss in entropy for the grafted arm vs the gain in conformational entropy for the free arms as the center of the star is pulled away from the surface. The tether serves as a "sacrificial arm" in order to minimize the free energy of the molecule as a whole.

The grafting density σ was found to have the most profound effect on the distribution of segments in the grafted layer. As the grafting density increases, the structure of the film gradually evolves to accommodate the free arms in the denser layer. Carignano and Szeifler hypothesized that at high grafting density, the two free arms of the branched polymers they investigated oriented antiparallel about the branch node, with one arm stretching toward the surface and one into the solvent.[22] This behavior is evidenced in Figures 1c and 2c for the many-arm stars as well. Even at moderate grafting densities, both the arms and arm ends partition between a dense region $z < z_{node}$ and a region of monotonically decreasing ϕ, $z > z_{node}$. This partitioning leads to a discontinuity seen in the total volume fraction profile at the layer where the monotonic and dense regions meet. Figures 1d and 2d clearly show a discontinuity in the volume fractions of arms in the layers above z_{node} and those below z_{node}. Arms stretching toward the grafting plane below the branch node are randomly arranged such that a nearly constant density of arm segments and end segments is maintained.

Effect of Arm Number. As observed by Cherepanova and Stekolnikov,[23] the structure of the grafted layer changes most dramatically with an increase from one to three or four arms. As the number of arms is increased beyond three or four, the polymers sufficiently lose their "linear" character and brushes formed by five-arm stars differ only quantitatively from eight- or twelve-arm stars. The grafting density necessary for strong partitioning of the arms and arm ends moves to lower values as the number of arms increases. Typical total volume fraction profiles for the case of five arms and ten arms are shown in Figures 1a and 2a, respectively.

Arms orienting away from the surface into the solvent are less confined and behave like a separate brush grafted to a "virtual surface" at the branch node. Support for this idea comes from Figure 3, which shows the layer height H (the first moment of the density distribution) as a function of the number of arms for $\sigma = 0.04$. The stars' arms are crowded at large f and will orient primarily toward the surface or the solvent with little lateral stretching. Because the tethered chain is maximally stretched at this grafting density for $f > 8$, the height of the brush will be controlled by the behavior of the chains stretching into the solvent as if a second surface existed at z_{node}. The height of the layer scales

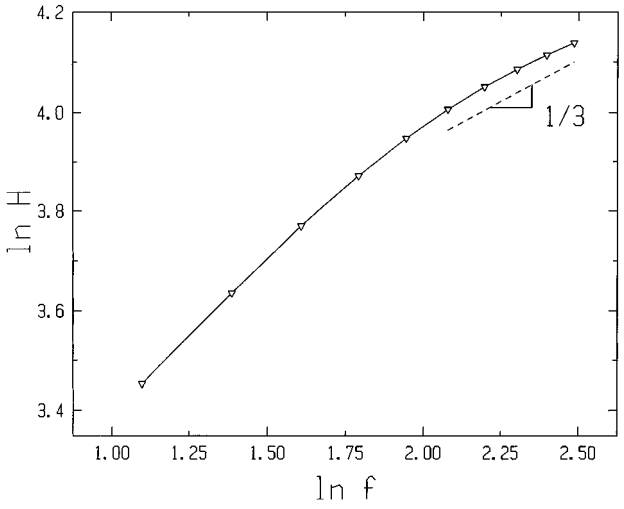

Figure 3. Monotonic layer height vs number of arms f per star. H is the height of the layer above the branch node at $z = z_{node}$. At constant grafting density, the slope is ~0.33 for $f > 8$.

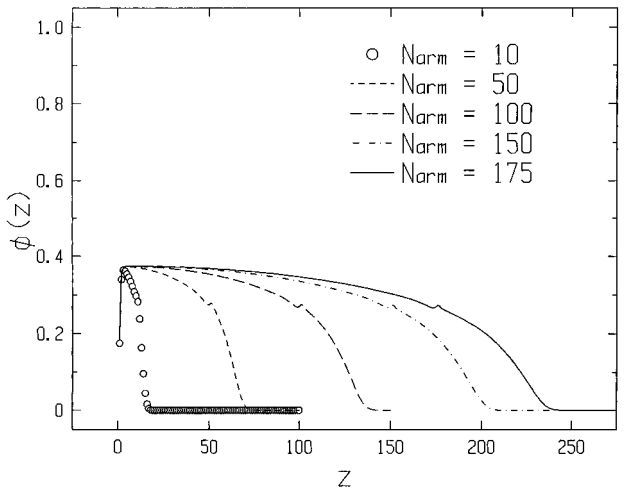

Figure 4. Total volume fraction profiles for grafted layers of eight-arm stars with one arm tethered to the surface. Each arm is the same length to give the total number of segments $N_{total} = fN_{arm} + 1$.

as $H \sim f^{1/3}$ for $f > 8$ at $\sigma = 0.04$. This is expected if the star arms are sufficiently crowded to orient like linear chains grafted at $z = z_{node}$. Then $\sigma = (nf)/A$ and $H \sim \sigma^{1/3}$, as predicted by Zhulina and Vilgis[27] for stars grafted to a surface by their center segment.

Effect of Star Size. The effect of the total number of segments on the volume fraction profile of the grafted layer is shown in Figure 4. The grafted layer profiles for stars having eight arms (one tethered) with $N_{arm} =$ 10−175 are calculated. The qualitative features shown by the arm ends, center segment, and total volume fraction profiles all vary smoothly as N_{total} ($=fN_{arm} +$ 1) is increased from 81 to 1401 with fixed grafting density $\sigma = 0.05$. The scaling dependence of the layer height with N_{total} obeys $H \sim N_{total}$, and the near surface volume fraction $\phi(z=3)$ is independent of N_{total}, as expected for linear chains.[8]

Bimodal Arm Stars. As mentioned above, the optimal concentration profile for a selective adhesion substrate is thought to have a high volume fraction of polymer near the surface and many end groups localized near the top of the grafted layer. With these criteria in mind, we investigated grafted layers of nine-arm stars having two different arm lengths. Five arms are

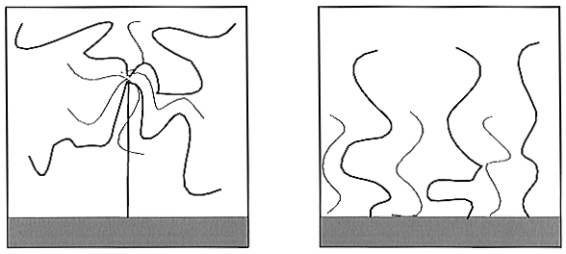

Figure 5. Schematic of bimodal grafted polymer layers: (a) bimodal stars; (b) bimodal linear chains.

100 segments in length, one of which is grafted to the surface, while the remaining four are 50 segments long. Figure 5 depicts schematically the system of interest, for the case of grafted bimodal stars and the corresponding case of a bimodal linear brush. Typical volume fraction profiles for this system are shown in Figure 6 for $\sigma = 0.06$. The total volume fraction profile is qualitatively similar to that for the case of uniform star arms for $z < z_{node}$. In the outer brush layer ($z > z_{node}$), however, the long and short chains appear to behave much like a bidisperse brush layer of linear chains. This is evidenced by comparing the stars with the corresponding bimodal linear brush shown in the insets of Figure 6. The bimodal linear brush depicted consists of 100-segment long chains and 50-segment short chains grafted at $\sigma = 0.05$ and 0.03, respectively, in accord with the density of arms stretching above the branch node in the star grafted layer.

Brush layers of linear chains having two different lengths have been investigated both analytically and via computer simulation.[18,21,30,31] The long and short chains segregate into distinct layers, creating a discontinuity in the first derivative of the volume fraction. The insets of Figures 6a and 6b depict the SCF results for the total volume fraction and separate long- and short-chain volume fractions of such a bimodal linear brush. The discontinuity also occurs in the monotonic region of the grafted star layer (Figures 6a and 6b). The qualitative similarity between the monotonic region of the star brush and the bimodal brush (at equivalent effective grafting density) is striking. The heights of the long and short chains (H_L and H_S) in a bidisperse linear chain brush layer have been previously characterized using two parameters, q and α, which are the number fraction of long chains and the fractional excess length $(N_L - N_S)/N_S$, respectively.[18] In the limit of strong stretching for both long and short arms, the scaling behavior of H_L and H_S with q and α are obtained as[30,31]

$$H_S = H_0(1 - q^{2/3})^{1/2} \qquad \text{(III.1)}$$

$$H_L = H_0(1 + \alpha q^{1/3}) \qquad \text{(III.2)}$$

where H_0 is the height of a monodisperse brush of chains of length N_S. For the case of bimodal arm stars investigated here, the scaling dependence of the height of the long and short arms with q and α follows (III.1) and (III.2), although H_S also shows a dependence on α as observed by Dan and Tirrell for bidisperse linear brush layers.[21] This result lends further support for the existence of a "virtual surface" at $z = z_{node}$.

In the bimodal arm star brush, the segment density distribution for the short arms has a maximum in the plane containing the branch node, suggesting that the short arms are partially oriented parallel to the surface. The segregation of the short arms is also accompanied

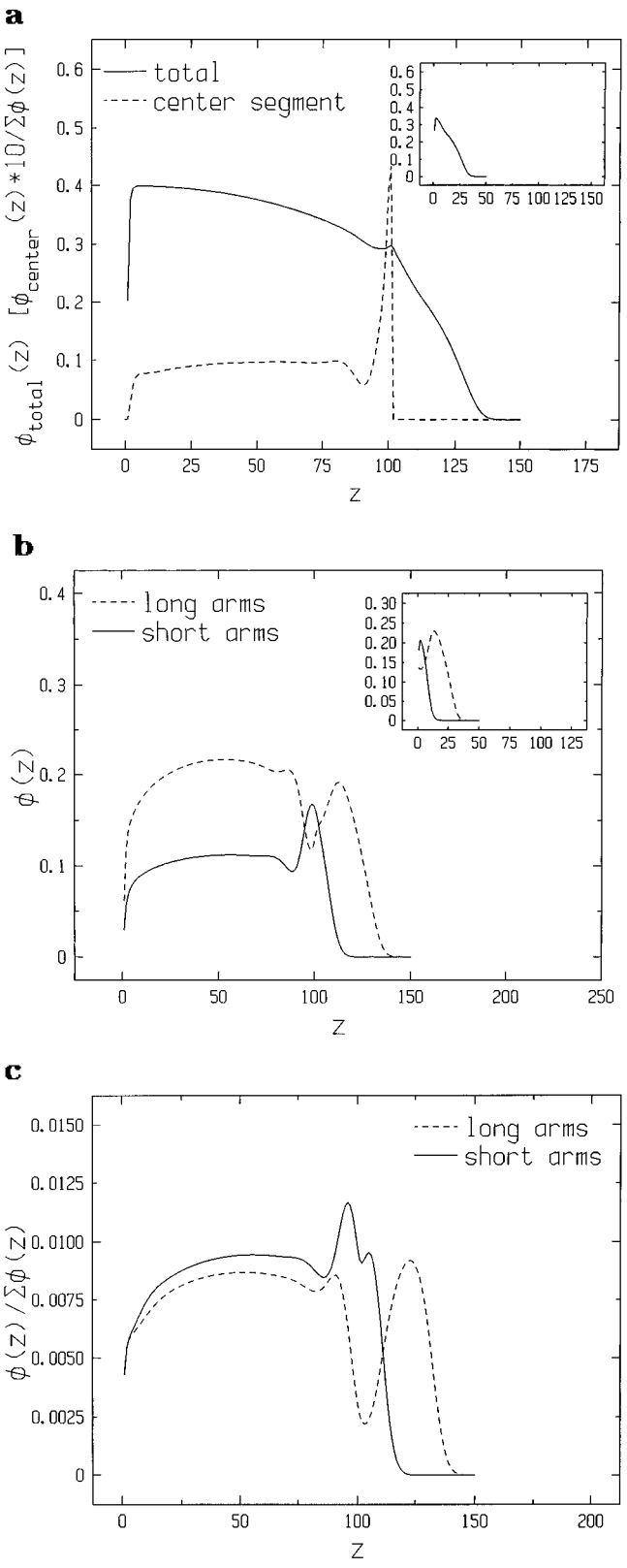

Figure 6. (a) Total and center segment volume fraction profiles for grafted layer of stars having a bimodal distribution of arm lengths, $\sigma = 0.06$. The inset shows a bimodal linear brush consisting of long and short chains at grafting densities equivalent to that of the star arms extending above the branch node. The total profile in the region $z > z_{node} = 101$ is very similar to that obtained for the bidispersed linear chain brush. (b) Long ($N_{arm} = 100$) and short ($N_{arm} = 50$) arm volume fraction profiles for the bimodal arm length grafted stars. The inset shows the corresponding calculations for the equivalent bimodal linear brush. (c) End segment volume fractions for the long and short arms of bimodal arm length grafted stars.

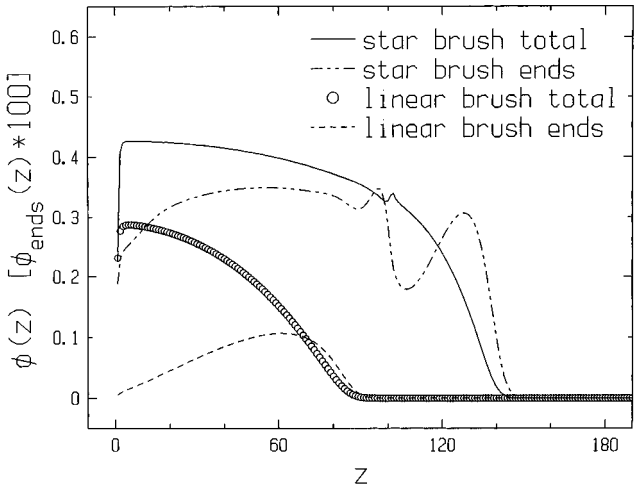

Figure 7. Volume fraction profiles for grafted layers of star and linear chain molecules. Comparison is made between a layer of eight-arm stars ($N_{arm} = 100$, $N_{total} = 801$) and a layer of linear chains ($N_{total} = 201$). Total and end segment volume fraction profiles are shown for $\sigma = 0.05$.

by localization of the short arm ends to the interface between the long and short arms in the region $z > z_{node}$.

Comparison of Linear and Star Polymer Brushes. Grafted layers of stars may be superior to grafted linear chains for preparing smart cell adhesion substrates. One of the challenges in designing such a surface with long-term stability using linear chains is to achieve a high surface coverage. Stars give higher surface coverage at any grafting density due to their bulkier structure. The high segment density in the layer achieved at moderate σ by grafted stars may be more effective for promoting protein resistance. Figure 7 compares the concentration profiles for the case of an eight-arm grafted star layer and a linear chain grafted layer. The degrees of polymerization were chosen to give equivalent ideal coil dimensions for each molecule. By choosing the same grafting density for both cases, this simulates the optimum surface coverage for linear and star molecules grafted covalently in a poor solvent assuming the same degree of overlap between the molecules in the ideal state. For the star molecules, the radius of gyration is given by

$$R_g^2 \sim (3f - 2)N/6f^2 \qquad \text{(III.3)}$$

and for linear chains

$$R_g^2 \sim N/6 \qquad \text{(III.4)}$$

The star molecule chosen is an eight-arm star with 100 segments per arm. This dictates a degree of polymerization $N = 275$ for the linear chain. The grafting density is $\sigma = 0.06$, giving an interchain distance in the ideal state of $d \approx 0.66R_g$. For the grafted star layer, the near surface volume fraction $\phi(z=3)$ is 1.48 times that of the linear brush.

Figure 7 also shows volume fraction profiles for the chain ends in each case. Many-arm stars have the advantage of multiple free ends which might be functionalized with specific ligands recognized by cells to promote cell adhesion. More chain ends are present per molecule in the star layer, and a significant fraction of these localize at the top of the brush layer. By contrast, the linear brush does not show strong localization of the ends at equal grafting densities.

IV. Conclusions

Grafted layers of star polymers show interesting structure at moderate grafting densities, experimentally accessible through control of grafting conditions. Arms partition into a dense region below the branch node and a monotonic region above it, creating a virtual surface at the node layer. When the arms of the stars are crowded, those arms stretched into the monotonic region control the height of the grafted layer, and the layer shows the same scaling of brush height with grafting density as linear chain brushes. The dense region shows a high concentration of segments relative to brushes of linear chains at the same grafting density, while the monotonic region also shows stronger localization of chain ends near the top of the layer than linear chain brushes at equal grafting density. This occurs due to the higher *effective* grafting density of star arms stretching from the branch node into the top of the layer. One may be able to exploit these differences to prepare substrates with improved resistance to protein adsorption and specific cell adhesion. Preparation of covalently bound grafted layers in poor solvent will give rise to much denser star surfaces as an end result of the stronger swelling effects of a good solvent on a star molecule vs a linear molecule and may create the kind of brush structure described above.

In addition, a bimodal distribution in the arm length of the stars leads to a maximum in the concentration profile of the short branches near the branch node, which may indicate lateral stretching of the short arms. Segregation within the upper layer of the brush obeys the scaling laws obtained for a bidisperse brush layer of linear chains, lending further support to the existence of a virtual surface at z_{node}.[18]

Further study of this system and other branched architectures is being pursued, including a systematic examination of the effect of solvent quality on the layer structure. The calculations are also being expanded to two dimensions to obtain information about the lateral order in grafted layers of star polymers and to guide the design of a surface with controlled receptor site distribution.

Acknowledgment. This work was supported in part by the National Science Foundation under Grant No. DMR-9357602.

References and Notes

(1) Harris, J. M., Ed. *Poly(ethylene glycol) Chemistry: Biotechnical and Biomedical Applications*; Plenum Press: New York, 1992.
(2) Heller, W.; Pugh, T. L. *J. Chem. Phys.* **1954**, *22*, 1778.
(3) Vincent, B. *Adv. Colloid Interface Sci.* **1974**, *4*, 193.
(4) Gersappe, D.; Irvine, D.; Balazs, A. C.; Rafailovich, M.; Sokolov, J.; Liu, Y.; Schwarz, S.; Pfeiffer, D. *Science* **1994**, *265*, 1072.
(5) Israels, R.; Gersappe, D.; Fasolka, M.; Roberts, V. A.; Balazs, A. C. *Macromolecules* **1994**, *27*, 6679.
(6) Jeon, S. I.; Andrade, J. D. *J. Colloid Interface Sci.* **1991**, *142* (1), 159.
(7) Milner, S. T. *Science* **1991**, *251*, 905.
(8) Milner, S. T.; Witten, T. A.; Cates, M. E. *Macromolecules* **1988**, *21*, 2610.
(9) Alexander, S. *J. Phys. (Paris)* **1977**, *38*, 983.
(10) de Gennes, P.-G. *J. Phys. (Paris)* **1976**, *37*, 1443. de Gennes, P.-G. *Macromolecules* **1980**, *13*, 1069.
(11) Mansfield, T. L.; Iyendar, D. R.; Beaucage, G.; McCarthy, T. J.; Stein, R. S.; Composto, R. J. *Macromolecules* **1995**, *28*, 492.
(12) Lai, P.; Binder, K. *J. Chem. Phys.* **1991**, *95* (12), 9288.
(13) Prime, K. L.; Whitesides, G. M. *J. Am. Chem. Soc.* **1993**, *115* (23), 10714.
(14) Scheutjens, J. M. H. M.; Fleer, G. J. *J. Phys. Chem.* **1979**, *83* (12), 1619.
(15) Cosgrove, T.; Heath, T.; Van Lent, B.; Leermakers, F.; Scheutjens, J. *Macromolecules* **1987**, *20*, 1692.
(16) Hirz, S., M.Sc. Thesis, University of Minnesota, 1987.
(17) Skvortsov, A. M.; Gorbunov, A. A.; Pavlushkov, I. V.; Zhulina, E. B.; Borisov, O. V.; Priamitsyn, V. A. *J. Colloid Interface Sci.* **1990**, *137*, 495; *Vysokomol. Soedin., Ser. A* **1988**, *31*, 1615.
(18) Lai, P.; Zhulina, E. B. *Macromolecules* **1992**, *25*, 5201.
(19) Brown, G.; Chakrabarti, A.; Marko, J. F. *Europhys. Lett.* **1994**, *25* (4), 239.
(20) Murat, M.; Grest, G. S. *Macromolecules* **1989**, *22*, 4504.
(21) Dan, N.; Tirrell, M. *Macromolecules* **1993**, *26*, 6467.
(22) Carignano, M. A.; Szleifer, I. *Macromolecules* **1994**, *27*, 702.
(23) Cherepanova, T. A.; Stekolnikov, A. V. *Mol. Phys.* **1994**, *83* (6), 1065.
(24) Siqueira, D. F.; Kohler, K.; Stamm, M. *Langmuir* **1995**, *11*, 3092.
(25) Ligoure, C.; Leibler, L. *J. Phys. (Paris)* **1990**, *51*, 1313.
(26) Milner, S. T. *Macromolecules* **1992**, *25* (20), 5487.
(27) Evers, O. A.; Scheutjens, J. M. H. M.; Fleer, G. J. *Macromolecules* **1990**, *23*, 5221.
(28) Daoud, M.; Cotton, J. P. *J. Phys. (Paris)* **1982**, *43*, 531.
(29) Zhulina, E. B.; Vilgis, T. A. *Macromolecules* **1995**, *28*, 1008.
(30) Milner, S. T.; Witten, T. A.; Cates, M. E. *Macromolecules* **1989**, *22*, 853.
(31) Birshtein, T. M.; Liatskaya, Y. V.; Zhulina, E. B. *Polymer* **1990**, *31*, 2185.

MA951903T